

Enhanced Performance and Analysis of F2DTC of Asynchronous Motor Drive with TDCMLI Adopting SVPWM

Hari Babu. CH, Pakkiraiah. B, Paul Ratnakanth. Pallam

Abstract: *This paper proposes a PIDTC and Type-2 fuzzy based DTC with asynchronous drive having three level diode clamped MLI using the SVPWM technique. However, PIDTC of asynchronous motor drive with three level diode clamped multilevel inverter produces a poor dynamic performance during starting, speed reversal and load perturbation conditions. Moreover PIDTC has considerable THD present in the current and also more distortion present in flux and torque. The above problems can be overcome by using type-2 fuzzy controllers instated of PI controllers with logical rules. The simulated results of F2DTC shows the better transient performance, less THD in current and poor distortion in torque and flux as differentiate to PIDTC.*

Index Terms: *Proportional integral direct torque control (PIDTC), Type-2 fuzzy direct torque control (F2DTC), Direct torque control (DTC), Space vector pulse width modulation (SVPWM), Three level diode clamped multilevel inverter (TDCMLI).*

I. INTRODUCTION

In recent years most of the industries are running with high efficiency and low production cost. This is possible when the increased power in electrical equipments and electrical m/c [1]. Generally, for the motion control to utilize the electrical drives. In modern days most of electrical power is taken by drives only. Basically the drives are classified into two categories. Those are DC drives and AC drives. Now in this universe ac drives are enhancing to very popular. Because asynchronous motor drives look like a rugged structure and good efficiency, so that asynchronous motor drive utilization goes on increasing [2].

Essentially two ways of speed control of asynchronous motor drives are available. Those are scalar speed control

approach and vector speed control approach. In case of scalar speed control, control the magnitude speed of voltage and frequency only. So that scalar control is used for steady state applications only but not in transient state. Hence scalar speed control approach is suitable for low speed operating conditions and but not used for long range of speed control. Sudden change in load and speed reversal conditions asynchronous motor parameters like torque and flux produces ripples. Those problems can be overcome by using vector speed control [3], [2]. Basically vector speed control approaches are classified into two ways. Those are field oriented control approach and conventional direct torque control. In case of field oriented control strategy controls the torque and flux of asynchronous motor indirectly. However this control strategy involves more number of transformations, so that cost of equipment is increased [4]. The above problems can be overcome by adopting conventional direct torque control strategy instated of FOC control strategy. CDTC with hysteresis control strategy give better performance of IM and less ripples present in flux and torque of IMD then the FOC. But, in the hysteresis control approach switching frequency gets continuously varying. However, to manufacture the filters in order to reduce the ripple content in the torque and flux of IM are very difficult. But to avoid the above drawback and gives enhancing analysis of IM, introduce the pulse with modulation techniques [5]. Using the SVPWM technique gives the more ripples in both torque and current, because it is valid till 0.78 modulation indexes. So that in order to avoid above problem consider the combination of SVPWM inverter, BCSVPWM1 and BCSVPWM2 with T2FC. Utilizing above combination gives better improvement in the dynamic performance and steady state performance of torque and current of IM. As compare to PI SVPWM and PI TPWM methods. Here DTC-SVPWM with fuzzy logic gives the good dynamic performance of IM [6-8].

Type-1 fuzzy logic controls are the 2D control with simple logical rules and it is used for small uncertainty. Whereas type-2 fuzzy logic controller are 3D control and it is used for large food uncertainty [9]. Generally, for the low voltage appliance use the two-level inverter coupled with IM, even not suitable for medium voltage appliance. Because there are some restrictions are present, those are high switching

Manuscript published on 30 March 2019.

*Correspondence Author(s)

Hari Babu. CH, M.Tech, Dept. of Electrical and Electronics Engineering, Koneru Lakshmaiah Education Foundation, Deemed to be University, Greenfields, Vaddeswaram, Guntur, India.

Dr. Pakkiraiah. B, Associate Professor & M. Tech coordinator, MIEEE, LMISTE & MIAENG, Dept. of Electrical and Electronics Engineering, Koneru Lakshmaiah Education Foundation Deemed to be University, Vaddeswaram, Guntur-522502 Andhra Pradesh, India.

Paul Ratnakanth. Pallam, M.Tech, Dept. of Electrical and Electronics Engineering, Koneru Lakshmaiah Education Foundation, Deemed to be University, Greenfields, Vaddeswaram, Guntur, India.

© The Authors. Published by Blue Eyes Intelligence Engineering and Sciences Publication (BEIESP). This is an [open access](https://creativecommons.org/licenses/by-nc-nd/4.0/) article under the CC-BY-NC-ND license <http://creativecommons.org/licenses/by-nc-nd/4.0/>

frequency, more switching losses, and high current/voltage stress, so that cost of the equipment is hiked [10]. The above restrictions can be overcome by introducing the multi-level inverters instead of two-level inverter. Generally, here diode clamped multilevel inverter is considered in view of this work and remaining two methods have restrictions in its usage. Hence DTC-SVPWM with multilevel diode clamped inverter using type-2 fuzzy logic control produces the good performance of IM and also distortions present in the flux and torque of IM is considered as the negligible distortions as differentiated with F1DTC [11-14]. Now the overall performance of system and controllers are increased by utilizing multilevel inverter with DCT-SVPWM using type-2 fuzzy logic control compared to conventional techniques [15].

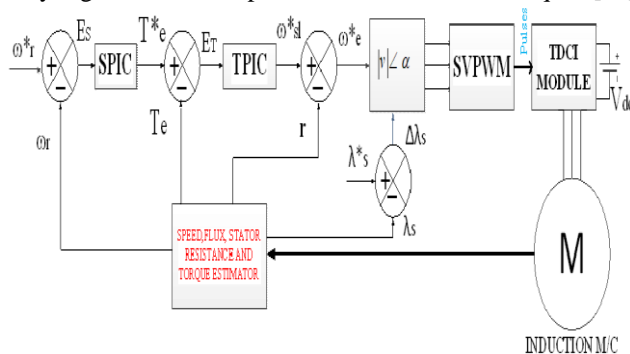


Fig. 1: Block Diagram of PIDTC of induction motor using TDCI

II. MATHEMATICAL MODELING OF DIRECT TORQUE CONTROL

Figure 1 represents the PIDTC of IM utilization TDCI. Estimate the rotor speed by compare through the reference speed via summation and that gives the error. Produce speed error is given to input of the SPIC, that reduces the error using the PI gain values. Similarly estimate the torque, flux and stator resistance of IM.

Expression for electromagnetic torque

$$\mathbf{T}_e = J \left(\frac{d\mathbf{n}}{dt} \right) + B \boldsymbol{\omega}_m + \mathbf{T}_L \quad (1)$$

Where J =Inertia constant, B =friction coefficient, T_L =Load torque

Electrical speed is two times of mechanical speed is shown in equation (2)

$$\omega_s = 2\omega_m \quad (2)$$

The estimated d-q axes stator flux is shown in equation (3) & (4)

$$\lambda_{as} = \int (v_{as} - i_{as} R_s) dt \quad (3)$$

$$\lambda_{ds} = \int (v_{ds} - i_{ds} R_s) dt \quad (4)$$

Here i_{qs} along with i_{ds} are denotes stator currents, v_{qs} as well as v_{ds} are denotes the stator voltages and R_s denotes stator resistance.

Therefore estimated stator flux can be written as below equation (5)

$$\lambda_s = \sqrt{\lambda_{ds}^2 + \lambda_{qs}^2} \quad (5)$$

The estimated stator resistance is

$$R_s = \frac{-3\omega_e T_e + \sqrt{(3\omega_e T_e)^2 + (2v_s i_s)^2 - (2\omega_e \lambda_s i_s)^2}}{2i_s^2} \quad (6)$$

The stator voltage and current are given by (7) & (8)

$$V_s = \sqrt{v_{ds}^2 + v_{qs}^2} \quad (7)$$

$$i_s = \sqrt{i_{ds}^2 + i_{qs}^2} \quad (8)$$

From the SPIC, reference electrical T_e^* torque is generated and estimated torque is given by

$$T_e = \frac{1.5P}{2} (\lambda_{ds} i_{qs} - \lambda_{qs} i_{ds}) \quad (9)$$

The calculated angle from the TPIC as

$$\theta = \int (\omega_{gl}^* + \omega_r) dt \quad (10)$$

The reference flux is estimated as

$$\lambda_s^* = |\lambda_s^*| \cos \theta + j |\lambda_s^*| \sin \theta \quad (11)$$

Change in stator flux linkage within d-q axes be given by

$$\Delta\lambda_{ds} = |\lambda_s^*| \cos \theta - \lambda_{ds} \quad (12)$$

$$\Delta\lambda_{gs} = |\lambda_s^*| \sin\theta - \lambda_{gs} \quad (13)$$

The reference voltages in $\alpha-\beta$ are calculated as

$$v_{\beta}^* = \left(\frac{\Delta \lambda_{qs}}{\Delta t} \right) + i_{qs} R_s \quad (14)$$

$$v_{\alpha}^* = \left(\frac{\Delta \lambda_{dx}}{\Delta t} \right) + i_{ds} R_s \quad (15)$$

The reference voltage can be represented in magnitude and angle format is given by

$$\bar{v}_r = |\sqrt{v_{\alpha}^{*2} + v_{\beta}^{*2}}| \angle \alpha \quad (16)$$

Here α represents the angle between reference voltage vector as well as A-phase vector. Therefore after estimation of magnitude and angle then generation of SVPWM pulses straightforwardly.

III. DESIGN OF SVPWM TECHNIQUE FOR TDCI

The figure 2 shows a three level inverter. Here p, o and n represent the positive, neutral and negative respectively. And corresponding pole voltages can be measured per phase, by conducting either top two switches or middle two switches or lower two switches must be on.

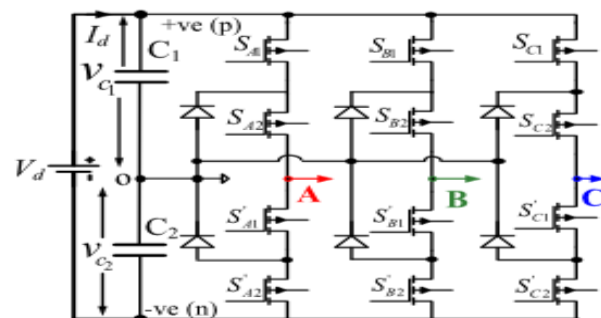



Fig. 2: Three level inverter

Therefore the respective per phase pole voltages (VAO, VBO, and VCO) are obtained as $+0.5V_d$, $0V_d$, and $-0.5V_d$, when A, B and C phases are connected to p, o and n respectively. Generally a 3-, three level diode clamped inverter carry total 27 switching states and they are shown in figure 3, in those 24 switching vectors are active state vectors and remaining 3 switching vectors are zero state vectors. Non-zero vectors are classified into small voltage vector, medium voltage vectors, and large voltage vectors are represented in figure x and corresponding magnitudes are $0.33V_d$, $0.5773V_d$, and $0.667V_d$.

Additionally active vectors are phase-displaced by 60° with respective their group of voltage vectors are shown in figure 3.

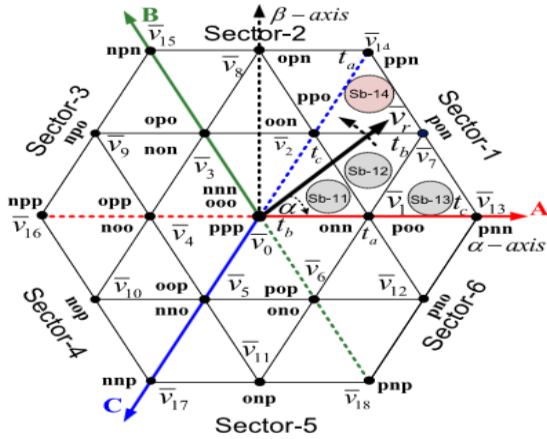


Fig. 3: Three level voltage vector representation

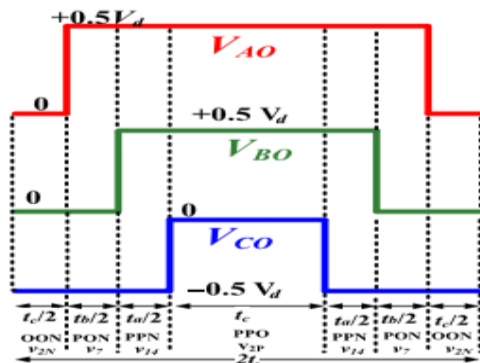
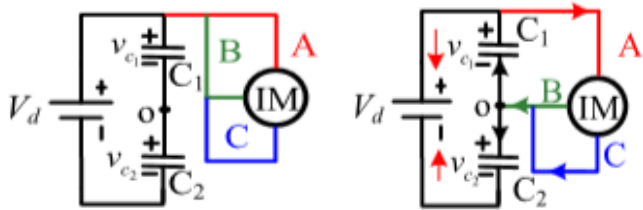
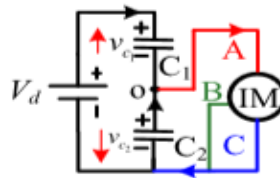


Fig. 4: Pole voltage representation of SVPWM

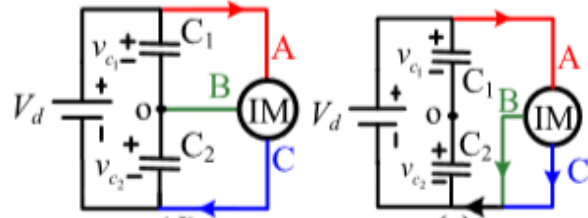
In general, capacitors (C1 and C2) in the TDCI faces voltage-balance problem so that output voltage decreases, increased switching stress, exceeds capacitor tolerance limits and output voltage gets distorted there by THD increases. Those draw backs can be overcome by using SVPWM algorithm. In which, the appropriate switching vector is selected based on the reference vector position without using an extra controller. Fig. 3 shows the effect of capacitor voltages for different switching vectors involved at the sector1 region. In case zero- and large-voltage vectors are shown in Fig. 3(a) and (e) in which there is no current flows through neutral point, and hence, capacitors are balanced. Fig. 3(b) belong to p-type small voltage vectors, then the capacitor c1 and c2 are discharging and charging respectively, moreover average voltage across capacitors vc1 and vc2 are will maintain constant such that there is no current flows through the neutral point. Similarly consider n-type small voltages are quite opposite to p-small voltage vectors. In case of medium-voltage vector direction of current flow current depends completely on load.



(a) Zero voltage vector (ppp) (b) p-type small vector (poo)



(c) n-type small vector (onn)



(d) Medium vectors (pon) (e) large vector (pnn)

Fig. 5: Effect of capacitor voltages for corresponding switching states.

Understanding the construction of three level SVPWM inverter is difficult as differentiate with the two level inverter. As same as two level inverter, pole voltage of three level SVPWM inverter are easily estimated by using single switching transition from one state to next state. Using two levels SVPWM to generalize three level SVPWM inverter, and these three level voltages are representing into six sectors. But every sector subdivided into 4-sectors as show in above figure. The reference vector is present on sub sector region-4 then volts-second balance principle is applied.

$$\vec{v}_r \angle \alpha^\circ t_s = \vec{v}_2 \angle 60^\circ t_a + \vec{v}_7 \angle 30^\circ t_b + \vec{v}_{14} \angle 60^\circ t_c \quad (17)$$

$$t_s/2 = t_a + t_b + t_c \quad (18)$$

$$t_a = 2t_s (k \sin \alpha - 0.5) \quad (19)$$

$$t_b = 2t_s k \sin(60^\circ - \alpha) \quad (20)$$

$$t_c = 2t_s (1 - k \sin(60^\circ + \alpha)) \quad (21)$$

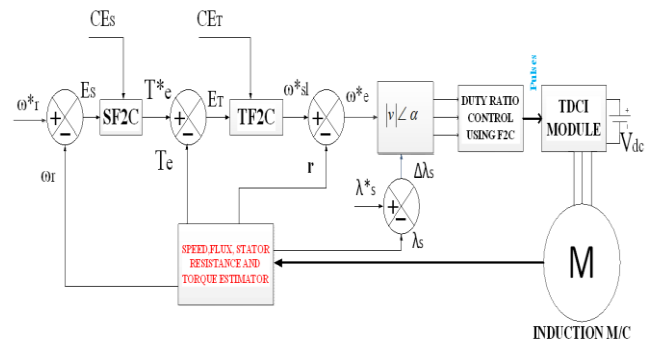


Fig. 6: BLOCK DIAGRAM FOR FUZZY-2 BASED DTC

IV. PROPOSED TYPE 2 FUZZY LOGIC BASED DTC

Generally artificial intelligence comes under the soft computer techniques, but artificial intelligence are majorly classified into fuzzy, ANN, and ANFIS etc. figure x represents the detail diagram of fuzzy-2 DTC. Here basically mamdani speed fuzzy-2 controller and mamdani torque fuzzy-2 DTC controllers are utilized.

The real values of speed lapse and difference in speed lapse are considered to be inputs of the speed fuzzy-2 controller, whereas real values of torque lapse and difference in torque lapse are considered to be inputs of torque fuzzy-2 controller. By using the above two controllers, generate required duty ratio pulses to TDCI [14]. Moreover utilizing of fuzzy-2 based DTC are gradually increased, because of their good dynamic performance of drive, less overshoots and fast rise time. Additionally fuzzy with DTC is independent of switching time period, so that to improve the firing range of inverters. A FLC converts crisps variables into linguistic control variables and fuzzy rules are constructed with help of expert knowledge or experience database. Generally with help of previews data base, to construct the fuzzy logic rules. Here seven levels of memberships are taken in order to obtain required crisp value [15]. Therefore the notations of membership functions and its names PL (positive large), PM (positive medium), PS (positive small), ZE (zero), NS (negative small), NM (negative medium) and NL (negative large) are shown in figure 11.

In generally, the characteristic of fuzzy controllers as follows

- 1) Input variables and output variables dependence of our requirement
- 2) Conversion of real values to fuzzy values
- 3) Inference engine
- 4) Conversion of fuzzy values to real values using centroid method.

The type-2 fuzzy set \bar{A} values view details in higher and lower membership functions

$$\bar{A} = \mu_{\bar{A}}(p, u) \quad (22)$$

Where $\mu_{\bar{A}}(p, u)$ is denotes the fuzzy-2 set values relating to real value position (p). In the fuzzification process real values are converted to fuzzy set values. And gathering of previews data is useful in field of developing membership functions of input. Therefore SPI controller produces T_e^* , and it is estimated as given below.

$$T_e^* = K_{ps} e_s^*(t) + K_{is} \int e_s^*(t) dt \quad (23)$$

Here K_{ps} denotes a proportional gain of speed fuzzy-2 controller K_{is} denotes an integral gain of speed fuzzy-2 controller and $e_s^*(t)$ is an error of SPIC. Applying differentiation of above equation on either side, we get

$$\frac{dT_e^*}{dt} = K_{ps} \frac{de_s^*(t)}{dt} + K_{is} e_s^*(t) \quad (24)$$

From above equation we can conclude differentiation of torque is directly proportional to speed error and change in speed error and they given by

$$E_s(K) = \omega_r^*(K) - \omega_r(K) \quad (25)$$

$$CE_s(K) = E_s(K) - E_s(K-1) \quad (26)$$

Where $\omega_r^*(K)$ and $\omega_r(K)$ are the orientation and real rotor speed, respectively. But here $E_s(k)$ denotes the instant speed error and $E_s(k-1)$ denotes the delay speed error

respectively. While a difference of torque $\Delta T_e^*(k)$ be generated from the speed regulator is

$$T_e^* = T_e^*(K-1) + \Delta T_e^*(K) \quad (27)$$

Where $T_e^*(K-1)$ is the instantaneous significance of the approximate torque value beginning the speed F2C (SF2C).

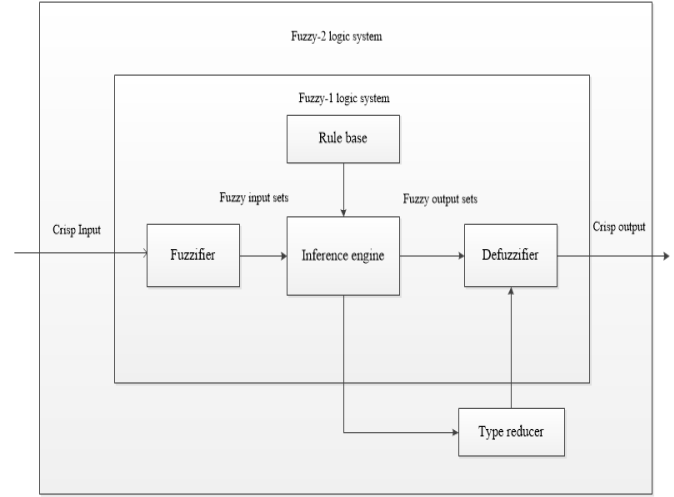


Fig. 7: Internal structure of F1C and F2C

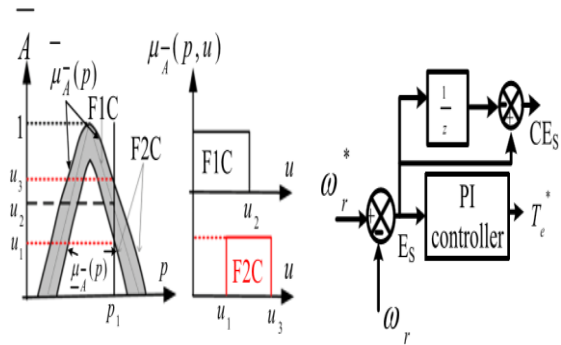


Fig. 8: Fuzzy-1 and fuzzy-2 MFs. Fuzzy set for F1C and F2C

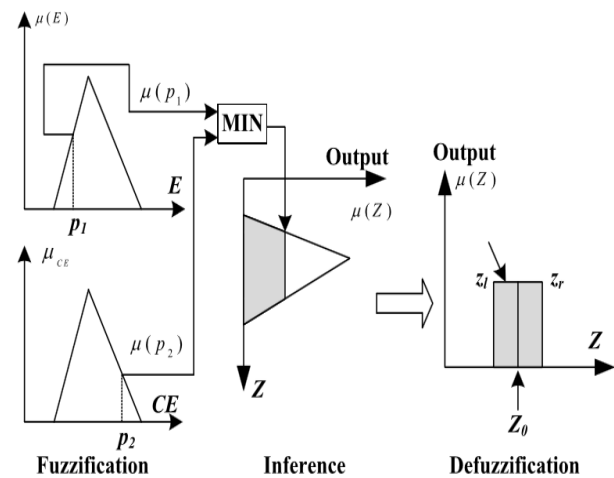


Fig. 9: Fuzzy-1 process

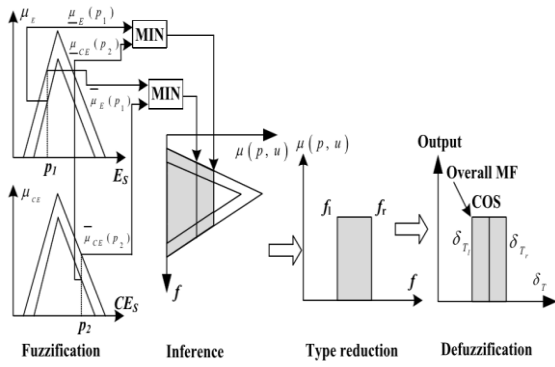


Fig. 10: Fuzzy-2 process

The output set analogous to every rule of the type-2 FLS be a type-2 set, the type drop combine each and every one these outputs in equivalent ways and subsequently perform centroid calculations taking place this type-2 set which lead towards type-1 set with the intention of we entitle the type-reduction set. Fuzzy-2 process has input and output MFs as shown above. Where the input membership functions are seven and output membership functions are also seven. Therefore they results the 49 possible rules. Those speed fuzzy-2 based rules are formulated in below tables. Similarly torque fuzzy-2 based rules are formulated.

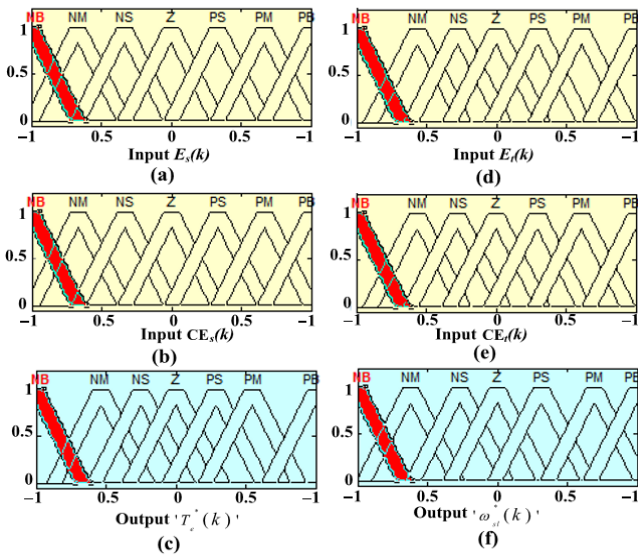


Fig. 11: Speed fuzzy-2 control: (a) error within $E_s(k)$; (b) change during error $CE_s(k)$; and (c) output torque. Torque fuzzy-2 control: (d) error within $E_t(k)$; (e) change during error $CE_t(k)$; and (f) output slip speed.

TABLE I. Rules for fuzzy-2 speed control

E_s CE_s	NB	NM	NS	Z	PS	PM	PB
NB	NB	NB	NB	NB	NM	NS	Z
NM	NB	NB	NB	NM	NS	Z	PS
NS	NB	NB	NM	NS	Z	PS	PM
Z	NM	NS	NS	Z	PS	PM	PB
PS	NM	NS	Z	PS	PM	PB	PB
PM	NS	Z	PS	PM	PB	PB	PB
PB	Z	PS	PM	PB	PB	PB	PB

The type-2 fuzzy set value of i^{th} regulation is able to be approximate like

$$F^i = (\underline{f}^i, \bar{f}^i) \quad (28)$$

$$\underline{f}^i = \underline{\mu}_{G_{E_s}}^i(E_s, u) * \underline{\mu}_{G_{CE_s}}^i(CE_s, u) \quad (29)$$

$$\bar{f}^i = \bar{\mu}_{G_{E_s}}^i(E_s, u) * \bar{\mu}_{G_{CE_s}}^i(CE_s, u) \quad (30)$$

Where $\underline{\mu}_{G_{E_s}}^i$ and $\bar{\mu}_{G_{CE_s}}^i$ are the results of lower along with upper membership functions.

Expression for interval fuzzy-2 set is

$$\delta_{T_{cos}} = (\delta_{T_l}, \delta_{T_r}) \quad (31)$$

Where $(\delta_{T_l}, \delta_{T_r})$ are denotes the left moreover right ending points.

Initially torque force is estimated as

$$\underline{f}^i \in F^i = (\underline{f}^i, \bar{f}^i)$$

Left end point can be formulated as

$$\delta_{T_l} = y_l = \sum_{i=1}^M [f_l^i y_l^i] / \sum_{i=1}^M f_l^i \quad (32)$$

Right end point can be formulated as

$$\delta_{T_r} = y_r = \sum_{i=1}^M [f_r^i y_r^i] / \sum_{i=1}^M f_r^i \quad (33)$$

Starting calculate the right end point δ_{T_r} and assume y_r^i is setup in ascending order

$$y_r^1 \leq y_r^2 \leq \dots y_r^M$$

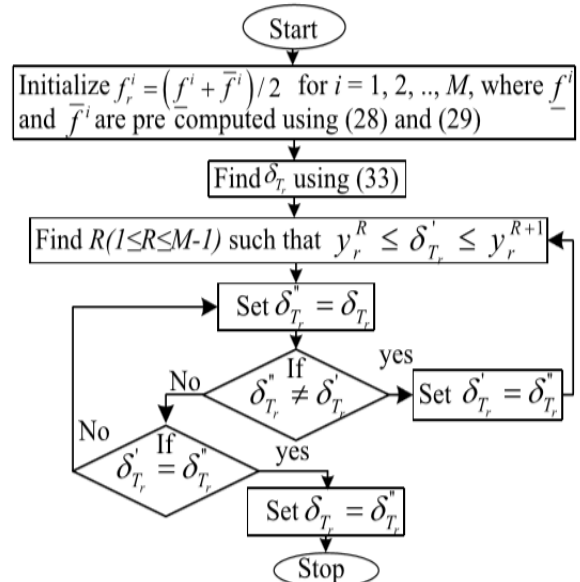


Fig. 12: Flow diagram for computing the real value of torque

Rearrange the expression for δ_{T_r} can be estimated

$$\delta_{T_r} = \delta_{T_r}(f^1, \dots, f^R, \bar{f}^{R+1}, \dots, \bar{f}^M, y_r^1, \dots, y_r^M)$$

$$= \left[\sum_{i=1}^R \underline{f}^i y_r^i + \sum_{i=R+1}^M \bar{f}^i y_r^i \right] / \left[\sum_{i=1}^R \underline{f}^i + \sum_{i=R+1}^M \bar{f}^i \right] \quad (34)$$

The same procedure is followed for finding the left end point δ_{T_l} . That can be express as

$$\delta_{T_l} = \delta_{T_l}(\bar{f}^1, \dots, \bar{f}^L, \underline{f}^{L+1}, \dots, \underline{f}^M, y_l^1, \dots, y_l^M)$$

$$= \left[\sum_{i=1}^L \bar{f}^i y_l^i + \sum_{i=L+1}^M \underline{f}^i y_l^i \right] / \left[\sum_{i=1}^L \bar{f}^i + \sum_{i=L+1}^M \underline{f}^i \right] \quad (35)$$

$$\delta_{T_{ec}} = (\delta_{T_r} + \delta_{T_l}) / 2 \quad (36)$$

$$\delta_{\omega_{slc}} = (\delta_{\omega_{slr}} + \delta_{\omega_{slc}}) / 2 \quad (37)$$

The above processor is same for the torque fuzzy-2 controller. Moreover input and output membership functions are also similar.

TABLE II. Rules for fuzzy-2 torque control

E_t	\rightarrow						
CE_t	NB	NM	NS	Z	PS	PM	PB
NB	NB	NB	NM	NM	NS	NS	Z
NM	NB	NM	NM	NM	NS	Z	PS
NS	NM	NM	NS	NS	Z	Z	PM
Z	NM	NS	NS	Z	Z	PS	PM
PS	NS	NS	Z	Z	PS	PM	PB
PM	NS	Z	Z	PS	PM	PM	PB
PB	PS	PS	PM	PM	PM	PB	PB

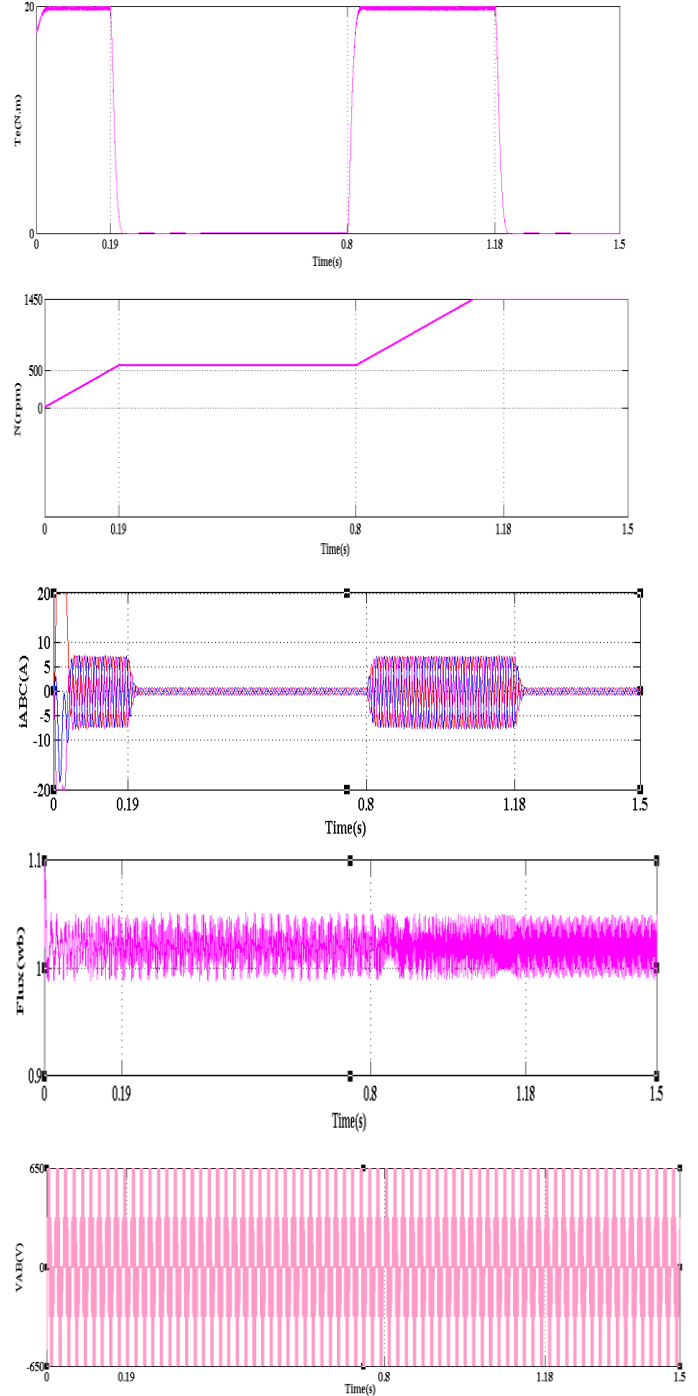
TABLE III. Duty ratios calculation at sector-1 region

Duty ratios	Subsectors in the sector-1 region			
	Sb-11	Sb-12	Sb-13	Sb-14
$d_a = t_a / 2t_s$	$0.5 - K \sin(60-\alpha)$	$0.5 - K \sin(\alpha)$	$1 - K \sin(60+\alpha)$	$K \sin(\alpha) - 0.5$
$d_b = t_b / 2t_s$	$0.5 - K \sin(60-\alpha)$	$K \sin(60-\alpha) - 0.5$	$K \sin(\alpha)$	$K \sin(60-\alpha)$
$d_c = t_c / 2t_s$	$K \sin(\alpha)$	$0.5 - K \sin(60-\alpha)$	$K \sin(60-\alpha) - 0.5$	$1 - K \sin(60+\alpha)$

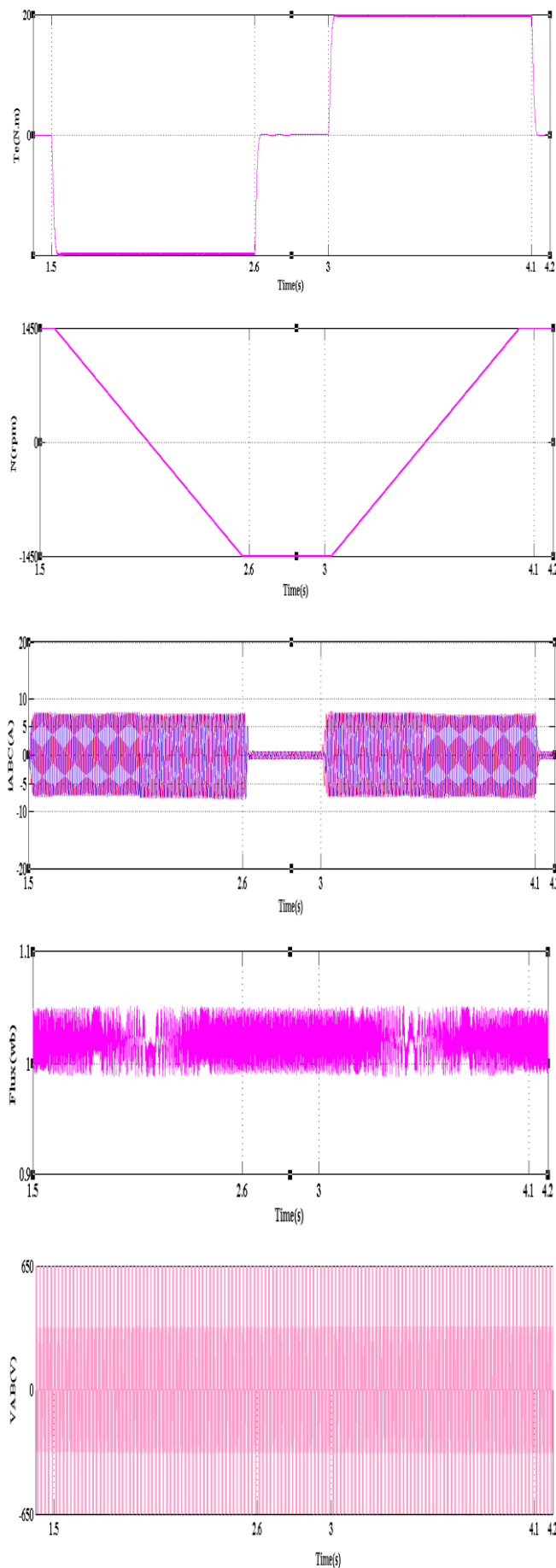
The advantages of making rules for type-2 fuzzy logic controller are less overshoot and fast rise time. Basically these rules are computed by relearned algorithm. Clearly observing the duty ratios of sector region-1 in the tabulation, duty ratios are independent of switching frequency. There by increasing the firing strength of inverter as differentiate to PIDTC.

V. RESULTS AND DISCUSSION

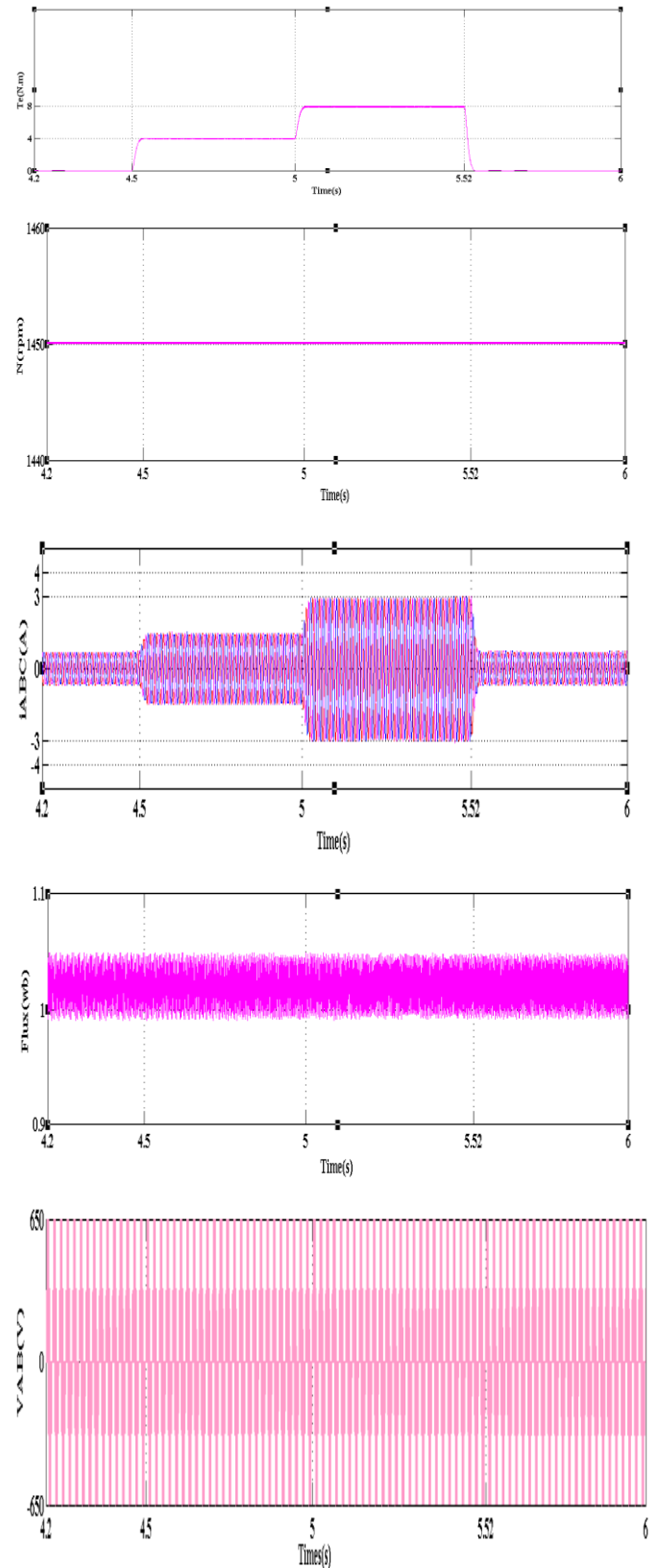
The simulated results for PITDC is taken in MATLAB is shown in below using three level diode clamped SVPWM inverter with switching frequency of 5kHz and made a time for sampling is 2μ sec for 2hp asynchronous motor. At starting reference speed is taken as 500 rpm until 0.8sec. After 0.8sec speed is step changed from 500 rpm to 1450 rpm with capacitor voltage of 650 volts. The other simulated results are speed (N_r), current (i_{ABC}), torque (T_e), flux and line to line voltage (V_{AB}) are given away in fig 13.



(i)

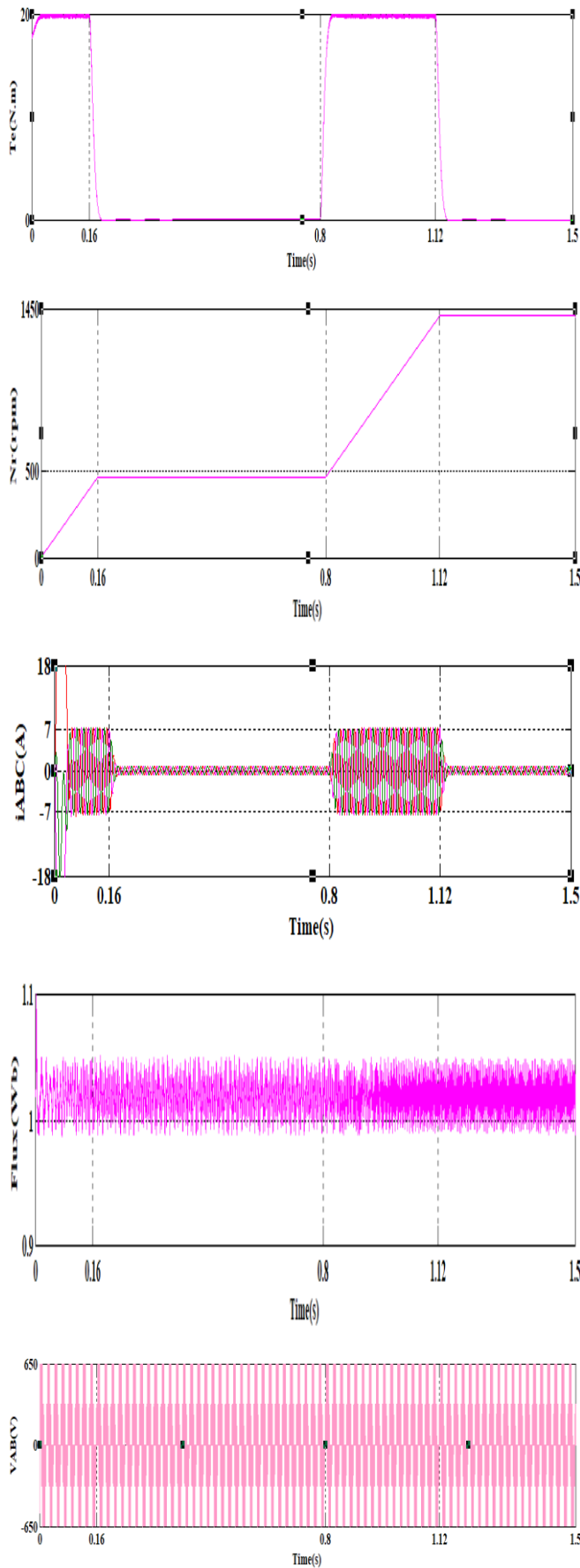


(ii)

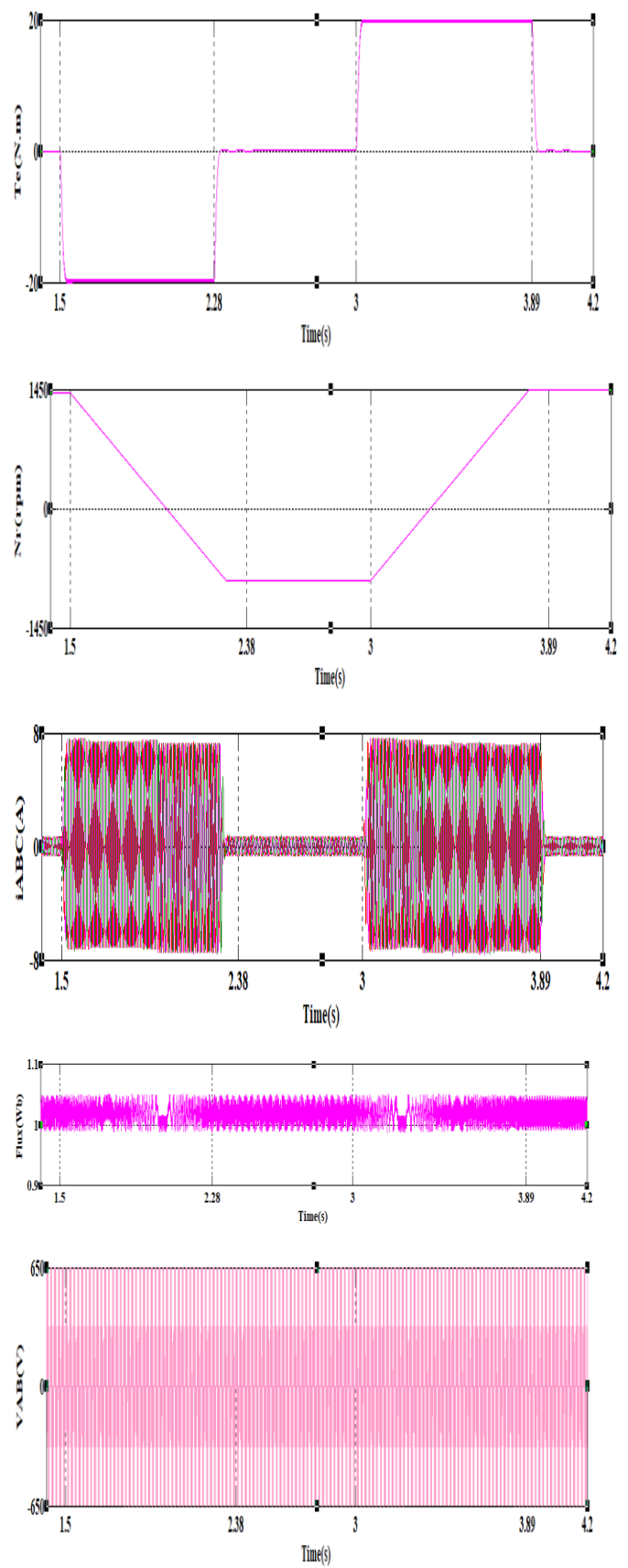


(iii)

Fig. 13: PIDTC of IM with Three level Inverter at (i) Starting, (ii) Speed reversal, and (iii) Load perturbation.



(i)



(ii)

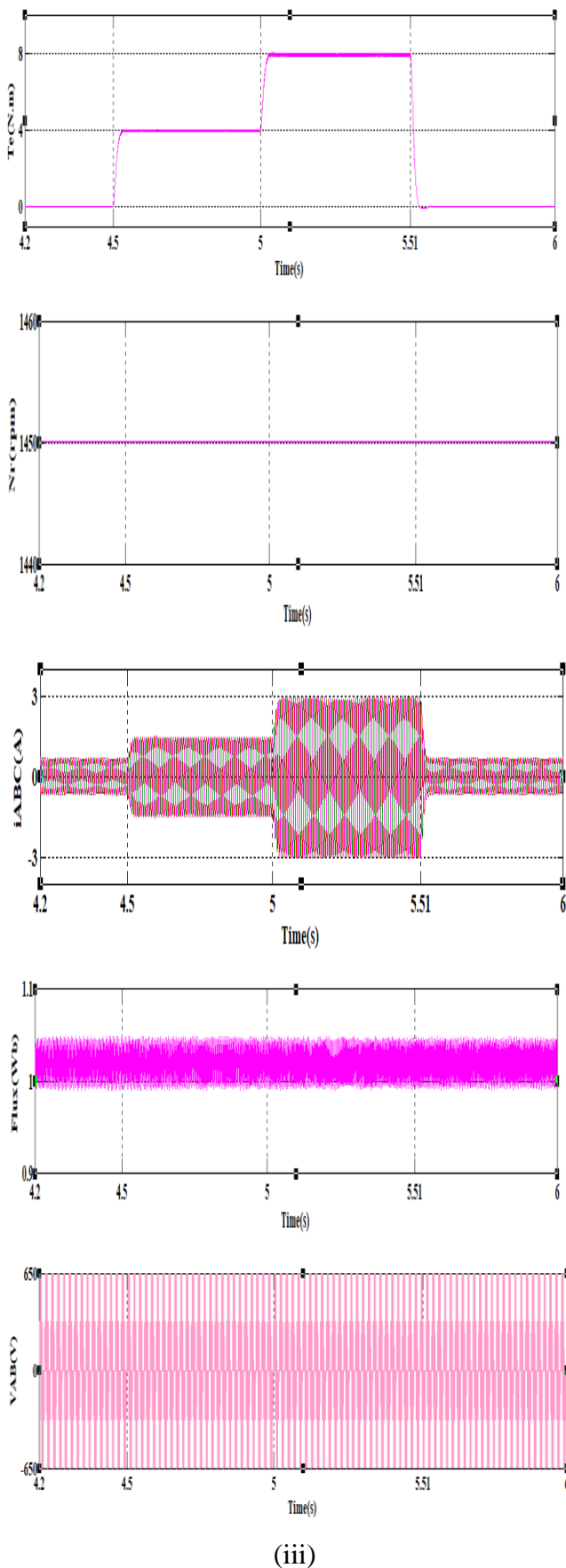


Fig. 14: F2DTC of IM with Three level Inverter at (i) Starting, (ii) Speed reversal, and (iii) Load perturbation.

Moreover voltage as well as flux is similar from initial to end. At 0.19sec current, torque in addition to speed be settled.

At 0.8sec speed goes to 500 rpm to 1450 rpm, in this time current, torque and flux gets distorted and they are settled at 0.18sec. At 1.5sec speed is start decreasing until it reaches to 0 rpm and after speed gets reverse direction. During that time magnitude of currents are high peaks. At 3sec again speed gets reversed, during that time currents and torque are also reversed. But flux and voltages are same from starting to ending. Load perturbation is applied at 4 N.m, 8 N.m and 0N.m. During that time magnitudes of current are different such as 0.7 A, 1.5 A and 2.9 A respectively. Likewise observing the simulated waveforms of F2DTC of Asynchronous motor in dissimilar functioning situations such as initial, step transform, speed setback and stack perturbation are shown in fig 14. The F2DTC takes less time to reach final value as differentiate with PIDTC. Moreover by observing the torque and flux waveforms of F2DTC then concluded that those waveforms have negligible distortions presented as differentiate with PIDTC. At no load, THD's of current for both PIDTC and F2DTC are 18.25% and 2.92% respectively. Hence considering all above parameters concluded that F2DTC of asynchronous motor gives improved performance than the PIDTC.

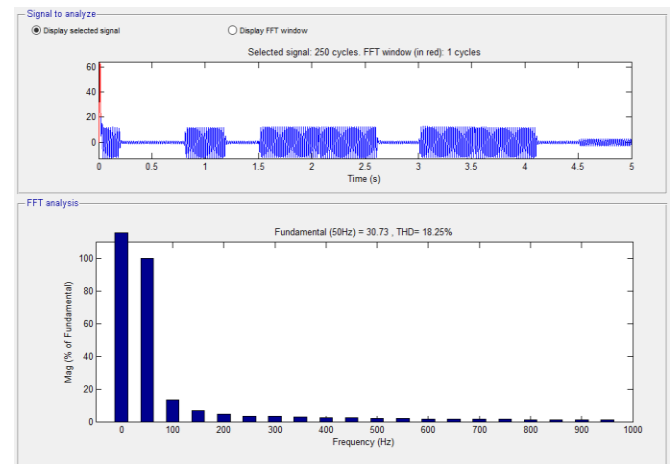


Fig. 15: Stator Current THD of IM with PIDTC

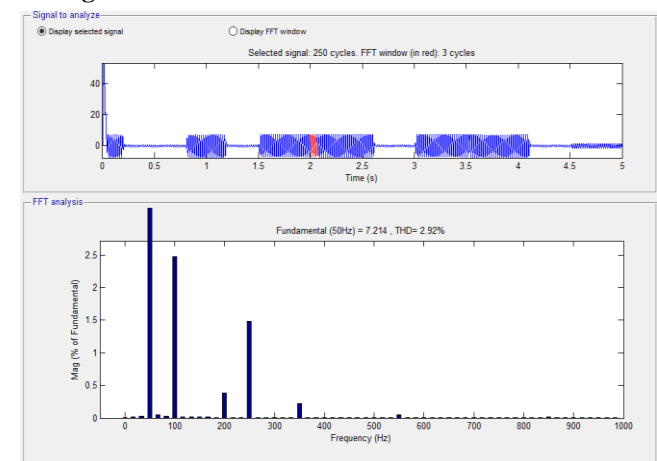


Fig. 16: Stator Current THD of IM with F2DTC

VI. CONCLUSION

In this paper comparison of simulated results for both PIDTC and F2DTC are taken in MATLAB with three level inverter of asynchronous motor drive using SVPWM technique. Moreover an appropriate voltage vector is selected using SVPWM technique; here to achieve unvarying voltage across the dc-link capacitors. In which F2DTC results less THD in current with differentiate to PIDTC. And also 3-level diode clamped multilevel inverter with F2DTC gives the good transient performance during starting, speed reversal and load perturbation. Moreover, F2DTC gives less distortion in torque as well as flux of asynchronous motor drive. The scope of the present theme is F2DTC with three level inverter of asynchronous motor. The comparison of F2DTC and ANFIS analysis will be do in further work.

REFERENCES

1. J. Rodriguez, S. Bernet, B.Wu, J.Pontt, and S.Kouro, "Multilevel voltage source-converter topologies for industrial medium-voltage drive," IEEE Trans. Ind. Electron., vol. 50, no. 6, pp. 2930-2945, Dec 2007.
2. B. K. Bose, (2002) "Modern Power Electronics and AC drive." innovative Jersey: Prentice Hall.
3. F., Blaschke. (1988). The principle of field-orientation as applied to the transvector closed-loop control system for rotating-field machines. Siemens Rev., vol. 34, pp. 135-147.
4. C. J. Bonanno, L. Zhen, and L. Xu, "A direct field oriented induction machine drive with robust flux estimator for position sensorless control," in Conf. Rec. IEEE-IAS Annu. Meeting, 1995, pp. 166-173.
5. J. Holtz and E. Bube, "Field oriented asynchronous pulse-width modulation for high performance ac machine drives operating at low switching frequency," IEEE Trans. Industry Applications, pp. 574-581, 1991.
6. T. Boller, J. Holtz, and A. K. Rthore, "Neutral point potential balancing using synchronous optimal pulse width modulation of multilevel inverters in medium voltage high power ac drives," in Proc. IEEE ECCE, Sep. 15-20, pp. 4802-4807.
7. J. M. D. Murphy and M. G. Egan, "A comparison of PWM strategies for inverter-fed induction motors," IEEE Trans. Industry Applications, pp. 363-369, 1983.
8. G. Narayanan, Di Zhao, Harish and K. Krishnamurthy, "Space Vector Based Hybrid PWM technique used for Reduced Current Ripple," IEEE Trans. On Ind. Electron, vol. 55, no.4, pp. 1614-1627, April 2008.
9. P. Vas, Sensorless Vector and direct Torque control. London-UK: Oxford University Press, 1998.
10. Zadeh, L.A.: 'Fuzzy sets' Inf. manage, 8, pp. 338-353.
11. M. J. Mendel, Uncertain rule-based fuzzy logic systems: Introduction and new directions. Prentice Hall PTR, Upper Saddle River, NJ, 2001.
12. Mendel, J. M.: "Type-2 fuzzy sets and systems: an overview", IEEE Comput. Intell. Mag., 2007, 2, pp. 20-29.
13. Mikkili, S., Panda, A.K.: 'PI and fuzzy logic controller base 3-phase 4-wire shunt active filter for mitigation of current harmonics with Id-Iq control strategy', J. Power Electron., 2011, 11, (6), pp. 914-921.
14. S. Mir, M. Elbuluk, and D. Zinger, "pi and fuzzy estimators for tuning the stator resistance in direct torque control of induction machines," IEEE Trans. Power Electron., vol. 13, pp. 279-287, Mar. 1998.
15. Nasir Uddin, M., and Hafeez, M., "FLC-based DTC system to improve the dynamic performance of an IM drive," IEEE Trans. Ind. Appl., vol. 48, pp. 823-831, March 2012.

AUTHORS PROFILE



Hari Babu. CH, received B.Tech degree in Electrical and Electronics Engineering in 2015. He is now pursuing M.Tech from Koneru Lakshmaiah Education Foundation deemed to be University in the department of Electrical and Electronics Engineering with specialization of Power Electronics and Drives. His research interests are Power Electronics and Drives and Power Electronic Converters.



Dr. Pakkiraiah B. received B. Tech. degree in Electrical and Electronics Engineering in 2010, M. Tech. degree in Power Electronics in 2013 and Ph. D. degree in 2017 with the specialization of Power Electronics & Drives in the department of Electrical and Electronics Engineering. He is the member of IEEE and life member of ISTE & IAENG. He is the recipient of "Best Young Scientist National Award". Presently he is working as Associate Professor & M. Tech

coordinator in the department of Electrical and Electronics Engineering at Koneru Lakshmaiah Education Foundation (Deemed to be University), Vaddeswaram, Guntur. His research interests are in power electronics and drives, neural networks and fuzzy logics and new research eras in renewable energy sources.



PAUL RATNAKANTH.PALLAM received his Bachelor's degree from KKR and KSR institute of technology and sciences which affiliated to JNTU-Kakinada in Electrical and Electronics Engineering in 2016. Presently an M.Tech research scholar in KLEF deemed to be university. His specialization is Power Electronics and Drives. His areas of interests are power electronics and drives, networks and electrical circuits, Artificial neural networks.

